Journal of
Mechanics of
Materials and Structures

THREE-DIMENSIONAL ISOFIELD MICROMECHANICS MODEL FOR EFFECTIVE ELECTROTHERMOELASTIC PROPERTIES OF PIEZOELECTRIC COMPOSITES

Santosh Kapuria and Poonam Kumari

Volume 6, No. 1-4 January–June 2011

mathematical sciences publishers

JOURNAL OF MECHANICS OF MATERIALS AND STRUCTURES
Vol. 6, No. 1-4, 2011

THREE-DIMENSIONAL ISOFIELD MICROMECHANICS MODEL FOR EFFECTIVE ELECTROTHERMOELASTIC PROPERTIES OF PIEZOELECTRIC COMPOSITES

SANTOSH KAPURIA AND POONAM KUMARI

A fully coupled three-dimensional micromechanics model based on the isofield method is developed for the effective electrothermoelastic properties of piezoelectric fiber-reinforced composite (PFRC) materials with poling and an electric field applied normal to the fiber direction. In the isofield method, the strain and electric field components parallel to the plane connecting two phases are assumed to be uniform across both phases, and likewise for the stress and electric displacement components normal to the connecting plane. The model employs the isofield assumptions for two possible connectivities, which are then combined so as to yield transverse isotropy of the effective properties when both constituents are transversely isotropic. The assumption of uniform electric field across two phases made by some existing theories can be achieved as a special case of the present formulation when the dielectric constants of the fiber and matrix phases are equal. The effects of the fiber volume fraction and dielectric ratio on the effective properties are studied for two PFRC systems, PZT-7A/epoxy and PZT-5H/epoxy. The results are compared with those available in the literature based on uniform electric field assumptions. It is found that the dielectric ratio has a very significant effect on the electromechanical and electrothermal coupling constants of PFRCs.

1. Introduction

Piezoelectric materials are being increasingly used as distributed sensors and actuators in structural health monitoring [Park et al. 2010] and control [Dong et al. 2006] applications. Their advantages over other available smart materials include easy commercial availability, efficient conversion of energy, relatively linear electromechanical behavior (at low fields), and large useful bandwidth [Chopra 2002]. However, for large-scale structural control applications such as in aerospace, automotive, and ship structures, monolithic piezoelectric actuators and sensors suffer from shortcomings with regard to tailorable anisotropic actuation, that is, directional actuation, robustness against damage during use and handling, ability to cover the entire structure for distributed actuation and sensing, and conformability to curved shell-type structural members. To address these concerns, piezoelectric fiber-reinforced composites (PFRCs) have been developed recently by embedding piezoceramic fibers in a resin matrix system, which, in addition to overcoming all the above-mentioned shortcomings, also possess higher specific stiffness, toughness, operating voltage range (from -1500 to $+2800$ V), and lifespan (200 million cycles) than the bulk material [Uchino 2000]. For designing such PFRC sensors and actuators as well as smart laminates integrated with these, it is necessary to have micromechanics models capable of estimating the effective electrothermoelastic properties of a unidirectional PFRC layer from the properties of its constituents.

Keywords: micromechanics, piezoelectric composite, electrothermoelastic, isofield method.

A number of micromechanics models have been proposed for piezoelectric composites in which the piezoelectric fibers are oriented along the thickness direction (Figure 1a). In this case, the poling and electric field directions are parallel to the fiber axis, causing a d_{33} effect, which is useful in ultrasonic transducer applications. These micromechanics models have been developed based on the Voigt-type isofield method [Chan and Unsworth 1989; Smith and Auld 1991], the Mori–Tanaka method [Dunn and Taya 1993], the self-consistent method [Dunn and Taya 1993; Levin et al. 2000], the generalized method of cells [Aboudi 1998], and the asymptotic homogenization method [Sabina et al. 2001; Levin et al. 2008].

Commonly used piezoelectric materials such as PZT and PVDF are transversely isotropic about their poling axes (class mm6 symmetry). Thus, when the piezoelectric fibers are aligned along the poling direction and the matrix is also transversely isotropic about the fiber direction, the transverse isotropy is retained in the composite system. All the above micromechanics models are thus concerned with transversely isotropic effective properties. In [Kar-Gupta and Venkatesh 2005], a unit cell-based finite element model was employed to obtain the electromechanical effective properties of a 1-3 piezoelectric composite system. In this system, the fibers are oriented along the thickness direction, while the fiber and matrix phases are poled along different directions (parallel or normal to the fiber direction) to generate a wide range of specific acoustic impedances.

For structural applications, however, the stiff piezoceramic fibers must be oriented in the plane of the structures (Figure 1b) and the poling as well as the electric field directions are perpendicular to the fiber axis, resulting in a d_{31} effect. In this case, the composite system is no longer transversely isotropic about the fiber axis, particularly with regard to the piezoelectric properties. Very few studies have been reported on the micromechanics of PFRC laminas of this type. The first such model was presented in [Bent 1994] using the isofield method for computing effective electroelastic properties. In that work, even though a general methodology was briefly outlined for calculation of effective material properties for the three-dimensional (3D) stress field considering two possible connectivity planes of the constituent phases, the detailed closed-form solutions and the results for effective material properties were presented by considering the uniaxial stress field only. The results for the 3D stress field based on this method have been presented only recently [Kapuria and Kumari 2010]. In [Mallik and Ray 2003;

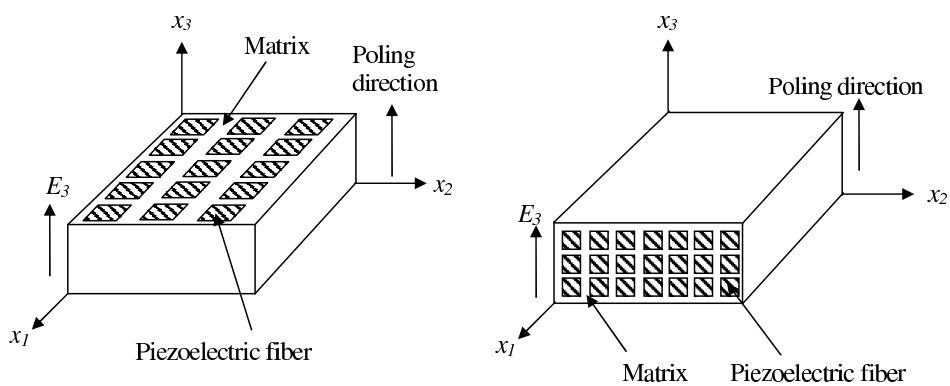

Figure 1. Schematic representation of PFRC with poling and electric field directions (a) parallel and (b) normal to fiber.

Ray 2006] a simpler model was presented using the uniform fields concept with a single connectivity plane (parallel to the fiber axis) for computing the effective electroelastic properties of PFRCs, which has been recently extended to the thermoelectroelastic case in [Kumar and Chakraborty 2009]. In this formulation, however, the electric field is assumed to be uniform across both the piezoelectric fiber and elastic matrix phases, which is not achievable when the electric field is applied across the thickness of the lamina, due to large difference in the dielectric constants of the two phases. The assumption is valid only when the two phases have the same dielectric constants, which is not the case for the materials commonly used for the purpose. Their formulation thus gives unrealistically high values (upper bounds) of the effective piezoelectric constants.

This paper presents a coupled 3D isofield model for estimating the effective electrothermoelastic properties of a unidirectional PFRC lamina with in-plane fibers and poling and electric field applied along the thickness direction. The effective properties are obtained for representative volume elements (RVEs) with two possible connectivity planes for the piezoelectric fiber and matrix phases, namely, parallel and normal to the fiber plane. The two models are combined in a way which maintains the transverse isotropy in the effective properties when both constituents are transversely isotropic about the fiber axis. Results are presented for two PFRC systems comprising, respectively, PZT-7A and PZT-5H fibers with an epoxy matrix. The results are compared with those of [Ray 2006; Kumar and Chakraborty 2009] obtained based on the uniform electric field assumption. The effect of the ratio of transverse dielectric constants of the fiber and matrix phases (hereafter called the dielectric ratio) on the effective piezoelectric and pyroelectric constants is illustrated. It is revealed that both effective piezoelectric and pyroelectric constants are maximal when the dielectric ratio is unity, and reduce drastically as the ratio increases. The effective thermoelastic properties are also compared with simplified models such as the rule of mixtures (ROM) and the modified rule of mixtures (MROM) [Gibson 2007] so as to ascertain their validity.

2. 3D isofield micromechanics model

2.1. ***Constitutive relations.*** The effective thermoelectroelastic constants of PFRC materials are determined from the properties of individual phases (fiber and matrix) by generalizing the 3D isofield approach of [Bent 1994; Kapuria and Kumari 2010] for the electrothermomechanical field. In order to have a unified treatment, both fiber and matrix are assumed to be piezoelectric materials, which are of orthotropic class mm2 symmetry, with principal material axes x_1, x_2, and x_3, and are polarized along the thickness direction x_3. The 3D linear constitutive equations of such a piezoelectric continuum are given by [Auld 1973]

$$\begin{bmatrix} \varepsilon_1 \\ \varepsilon_2 \\ \varepsilon_3 \\ \gamma_{23} \\ \gamma_{31} \\ \gamma_{12} \\ D_1 \\ D_2 \\ D_3 \end{bmatrix} = \begin{bmatrix} s_{11} & s_{12} & s_{13} & 0 & 0 & 0 & 0 & 0 & d_{31} \\ s_{12} & s_{22} & s_{23} & 0 & 0 & 0 & 0 & 0 & d_{32} \\ s_{13} & s_{23} & s_{33} & 0 & 0 & 0 & 0 & 0 & d_{33} \\ 0 & 0 & 0 & s_{44} & 0 & 0 & 0 & d_{24} & 0 \\ 0 & 0 & 0 & 0 & s_{55} & 0 & d_{15} & 0 & 0 \\ 0 & 0 & 0 & 0 & 0 & s_{66} & 0 & 0 & 0 \\ 0 & 0 & 0 & 0 & d_{15} & 0 & \epsilon_{11} & 0 & 0 \\ 0 & 0 & 0 & d_{24} & 0 & 0 & 0 & \epsilon_{22} & 0 \\ d_{31} & d_{32} & d_{33} & 0 & 0 & 0 & 0 & 0 & \epsilon_{33} \end{bmatrix} \begin{bmatrix} \sigma_1 \\ \sigma_2 \\ \sigma_3 \\ \tau_{23} \\ \tau_{31} \\ \tau_{12} \\ E_1 \\ E_2 \\ E_3 \end{bmatrix} + \begin{bmatrix} \alpha_1 \\ \alpha_2 \\ \alpha_3 \\ 0 \\ 0 \\ 0 \\ 0 \\ 0 \\ q_3 \end{bmatrix} T, \tag{1}$$

where ε_i and γ_{ij} denote the normal and shearing strain components, σ_i and τ_{ij} denote the normal and shear stress components, D_i denotes the electric displacements, E_i denotes the electric field components in the principal material axis system, and T denotes the temperature change over the reference stress-free temperature. Constants s_{ij}, d_{ij}, ϵ_{ij}, α_i, and q_3 are the elastic compliances, piezoelectric strain constants, dielectric constants, thermal expansion coefficients and pyroelectric constant, respectively.

The physical background of the isofield micromechanics model including its assumptions is described in Appendix A. In the generalized 3D isofield approach, the effective properties are first obtained for RVEs of two possible connectivities for the piezoelectric fiber and matrix phases: models A and B with material connectivity on the x_1-x_2 and x_1-x_3 planes respectively, as shown in Figure 2. The strain and electric field components parallel to the connecting plane of the two phases in a given RVE are assumed to be uniform across both phases (isofield condition), while isostress and isoelectric displacement conditions are assumed to exist along the direction normal to the connecting plane. The computations for the effective properties for the two models A and B are described below followed by the procedure of combining the two.

2.2. ***Model A.*** In model A, the connecting plane is x_1-x_2, and hence the strain components (ε_1, ε_2, γ_{12}) and electric field components (E_1, E_2) which are parallel to the connecting plane are assumed to be uniform across both phases, and isostress and isoelectric displacement conditions are assumed to exist

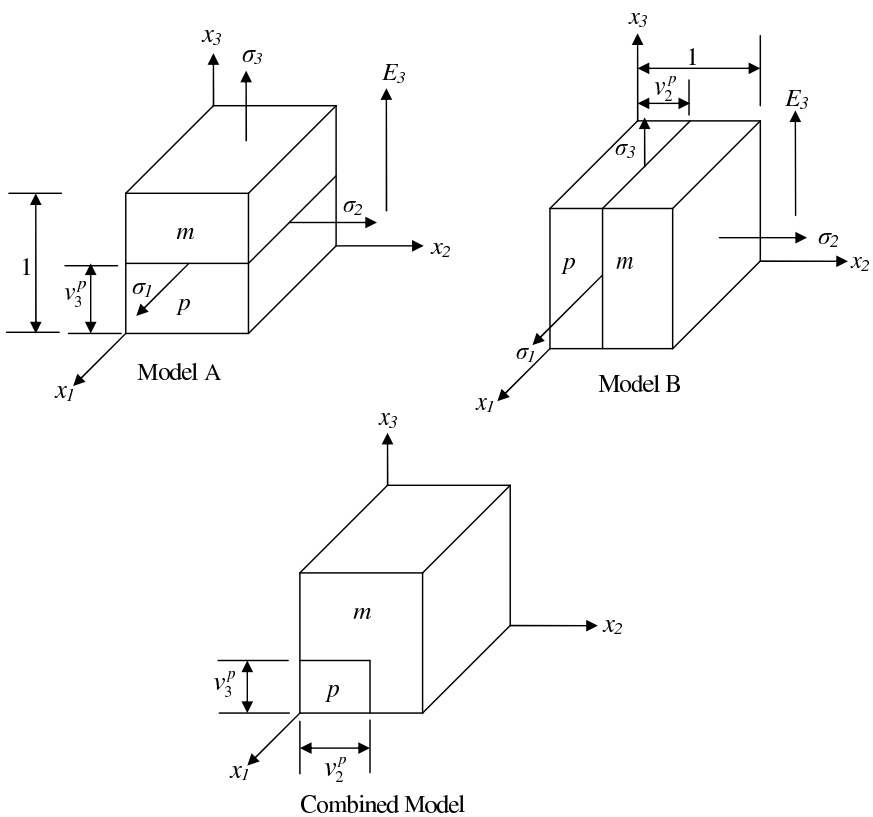

Figure 2. RVEs for isofield model (p: piezoceramic, m: matrix).

for $(\sigma_3, \tau_{23}, \tau_{13})$ and D_3, which are normal to the connecting plane. The electric field is considered to be applied along the thickness direction only, and the in-plane electric field components that may be used due to direct piezoelectric effect is neglected being small in comparison to E_3, that is, $E_1 \simeq E_2 \simeq 0$. It follows from (1) that, for this case, γ_{31} and γ_{12} become electromechanically uncoupled and hence the expressions for the effective shear compliances s_{55} and s_{66} (both normal to the fiber axis) will be similar. Hence, only one strain components γ_{12} is included in the following derivation, without any loss in generality. Thus, the isofield conditions for this case can be written as

$$\bar{U}^a = U_p^a = U_m^a \quad \text{with} \quad U^a = \left[\varepsilon_1, \varepsilon_2, \sigma_3, \tau_{23}, \gamma_{12}, D_3\right]^{\mathrm{T}}. \tag{2}$$

The superscript a corresponds to model A. An overbar denotes the average value, and subscripts p and m (also used as superscripts elsewhere) denote piezoelectric fiber and matrix phases, respectively. Temperature change is assumed to be uniform over fiber and matrix phases, that is, $\bar{T} = T_p = T_m$. The average value of the complimentary field components σ_1, σ_2, ε_3, γ_{23}, τ_{12}, and E_3 will have contributions from each phase in proportion to their volume fractions v_3^p and $v_3^m (= 1 - v_3^p)$ measured along the x_3 direction:

$$\bar{V}^a = v_3^p V_p^a + v_3^m V_m^a \quad \text{with} \quad V^a = \left[\sigma_1, \sigma_2, \varepsilon_3, \gamma_{23}, \tau_{12}, E_3\right]^{\mathrm{T}}. \tag{3}$$

The dependent field variables V^a can be expressed in terms of the independent variables U^a using the constitutive equation (1) as

$$V_\gamma^a = A^\gamma U_\gamma^a + A_t^\gamma \bar{T} \quad \text{with} \quad A^\gamma = \begin{bmatrix} a_{11} & -a_{12} & a_{13} & 0 & 0 & a_{16} \\ -a_{12} & a_{22} & a_{23} & 0 & 0 & a_{26} \\ -a_{13} & -a_{23} & a_{33} & 0 & 0 & a_{36} \\ 0 & 0 & 0 & a_{44} & 0 & 0 \\ 0 & 0 & 0 & 0 & a_{55} & 0 \\ a_{16} & a_{26} & -a_{36} & 0 & 0 & a_{66} \end{bmatrix}^\gamma, \quad A_t^\gamma = \begin{bmatrix} a_{t1} \\ a_{t2} \\ a_{t3} \\ 0 \\ 0 \\ a_{t6} \end{bmatrix}^\gamma, \tag{4}$$

where $\gamma = p, m$ and the constants a_{ij}^γ and a_{tj}^γ are given by

$$\begin{gathered}
a_{11}^\gamma = \frac{s'_{22}}{\delta}, \quad a_{12}^\gamma = \frac{s'_{12}}{\delta}, \quad a_{13}^\gamma = p_2^s, \quad a_{16}^\gamma = p_2^d, \quad a_{22}^\gamma = \frac{s'_{11}}{\delta}, \quad a_{23}^\gamma = p_1^s, \quad a_{26}^\gamma = p_1^d, \\
a_{33}^\gamma = p_2^s s'_{13} + p_1^s s'_{23} + s_{33} - d_{33} d'_{33}, \quad a_{36}^\gamma = p_2^d s'_{13} + p_1^d s'_{23} + d'_{33}, \quad a_{44}^\gamma = s_{44}, \quad a_{55}^\gamma = \frac{1}{s_{66}}, \\
a_{66}^\gamma = -p_2^d d'_{31} - p_1^d d'_{32} + \frac{1}{\epsilon_{33}}, \quad d'_{3j} = \frac{d_{3j}}{\epsilon_{33}}, \quad s'_{ij} = s_{ij} - d_{3i} d'_{3j}, \quad \delta = s'_{11} s'_{22} - {s'_{12}}^2, \\
a_{t1}^\gamma = p_2^t, \quad a_{t2}^\gamma = p_1^t, \quad a_{t3}^\gamma = p_3^t, \quad a_{t6}^\gamma = p_6^t, \quad \alpha'_j = \alpha_j - d'_{3j} q_3, \\
p_3^t = s'_{13} p_2^t + s'_{23} p_1^t + \alpha'_3, \quad p_6^t = -d'_{31} p_2^t - d'_{32} p_1^t - \frac{q_3}{\epsilon_{33}}, \quad p_i^t = (s'_{i1} \alpha'_2 - s'_{2i} \alpha'_1) \frac{(-1)^i}{\delta}, \\
p_i^s = (s'_{i1} s'_{23} - s'_{2i} s'_{13}) \frac{(-1)^i}{\delta}, \quad p_i^d = (s'_{i1} d'_{32} - s'_{2i} d'_{31}) \frac{(-1)^i}{\delta}, \quad i = 1, 2, \quad j = 1, 2, 3.
\end{gathered} \tag{5}$$

Substituting (4) for $\gamma = p$ and m into (3) and applying (2) yields

$$\bar{V}^a = (v_3^p A^p + v_3^m A^m) \bar{U}^a + (v_3^p A_t^p + v_3^m A_t^m) \bar{T} = A \bar{U}^a + A_t \bar{T}, \tag{6}$$

and therefore

$$\bar{U}^a = \hat{A}\bar{V}^a + \hat{A}_t\bar{T}, \qquad \hat{A} = A^{-1}, \qquad \hat{A}_t = -A^{-1}A_t. \tag{7}$$

Rearranging (7) in the form of (1), the effective constitutive equation and hence the effective material properties of PFRC for model A are obtained as

$$\begin{bmatrix} \bar{\varepsilon}_1 \\ \bar{\varepsilon}_2 \\ \bar{\varepsilon}_3 \\ \bar{\gamma}_{23} \\ \bar{\gamma}_{12} \\ \bar{D}_3 \end{bmatrix} = \begin{bmatrix} s_{11} & s_{12} & s_{13} & 0 & 0 & d_{31} \\ s_{12} & s_{22} & s_{23} & 0 & 0 & d_{32} \\ s_{13} & s_{23} & s_{33} & 0 & 0 & d_{33} \\ 0 & 0 & 0 & s_{44} & 0 & 0 \\ 0 & 0 & 0 & 0 & s_{66} & 0 \\ d_{31} & d_{32} & d_{33} & 0 & 0 & \epsilon_{33} \end{bmatrix}^A \begin{bmatrix} \bar{\sigma}_1 \\ \bar{\sigma}_2 \\ \bar{\sigma}_3 \\ \bar{\tau}_{23} \\ \bar{\tau}_{12} \\ \bar{E}_3 \end{bmatrix} + \begin{bmatrix} \alpha_1 \\ \alpha_2 \\ \alpha_3 \\ 0 \\ 0 \\ q_3 \end{bmatrix}^A \bar{T}, \tag{8}$$

where s_{ij}^A, d_{ij}^A, ϵ_{33}^A, α_i^A, and q_3^A are the effective material properties for model A, given by

$$\begin{aligned} &s_{i3}^A = \hat{a}_{i3}/\hat{a}_{33}, && s_{33}^A = 1/\hat{a}_{33}, && d_{33}^A = \hat{a}_{36}/\hat{a}_{33}, \\ &s_{ij}^A = \hat{a}_{ij} - s_{i3}^A s_{j3}^A/s_{33}^A, && && d_{3j}^A = \hat{a}_{6j} - d_{33}^A s_{j3}^A/s_{33}^A, && \text{for } i, j = 1, 2, \\ &s_{44}^A = 1/\hat{a}_{44}, && s_{66}^A = \hat{a}_{55}, && \epsilon_{33}^A = \hat{a}_{66} - (d_{33}^A)^2/s_{33}^A, \\ &\alpha_1^A = \hat{a}_{t1} - \hat{a}_{13}\hat{a}_{t3}/\hat{a}_{33}, && && \alpha_2^A = \hat{a}_{t2} - \hat{a}_{23}\hat{a}_{t3}/\hat{a}_{33}, \\ &\alpha_3^A = -\hat{a}_{t3}/\hat{a}_{33}, && && q_3^A = \hat{a}_{t6} - \hat{a}_{63}\hat{a}_{t3}/\hat{a}_{33}. \end{aligned} \tag{9}$$

2.3. ***Model B.*** In this case, the connecting plane being $x_1 - x_3$, the isofield condition over both phases is assumed to exist for ε_1, σ_2, ε_3, τ_{23}, γ_{31}, τ_{12}, and E_3, and their complimentary counterparts, σ_1, ε_2, σ_3, γ_{23}, τ_{23}, γ_{12}, and D_3 are averaged over the two phases

$$\bar{U}^b = U_p^b = U_m^b, \qquad U^b = \left[\varepsilon_1, \sigma_2, \varepsilon_3, \tau_{23}, \tau_{12}, E_3\right]^{\mathrm{T}}, \tag{10}$$

$$\bar{V}^b = v_2^p V_p^b + v_2^m V_m^b, \qquad V^b = \left[\sigma_1, \varepsilon_2, \sigma_3, \gamma_{23}, \gamma_{12}, D_3\right]^{\mathrm{T}}, \tag{11}$$

where v_2^p is the volume fraction of the fiber phase measured in model B along the x_2 direction (see Figure 2) and $v_2^m = 1 - v_2^p$. Using the constitutive equation (1), the dependent variables V_γ^b can be expressed in terms of the independent variables U_γ^b as

$$V_\gamma^b = B^\gamma U_\gamma^b + B_t^\gamma \bar{T} \quad \text{with} \quad B^\gamma = \begin{bmatrix} b_{11} & -b_{12} & b_{13} & 0 & 0 & -b_{16} \\ b_{12} & b_{22} & b_{23} & 0 & 0 & b_{26} \\ b_{13} & -b_{23} & b_{33} & 0 & 0 & -b_{36} \\ 0 & 0 & 0 & b_{44} & 0 & 0 \\ 0 & 0 & 0 & 0 & b_{55} & 0 \\ b_{16} & b_{26} & b_{36} & 0 & 0 & b_{66} \end{bmatrix}^\gamma, \quad B_t^\gamma = \begin{bmatrix} b_{t1} \\ b_{t2} \\ b_{t3} \\ 0 \\ 0 \\ b_{t6} \end{bmatrix}^\gamma, \tag{12}$$

where $\gamma = p, m$ and the elements b_{ij}^{γ} and b_{tj}^{γ} are given by

$$\begin{aligned}
b_{11}^{\gamma} &= s_{33}/\delta_1, & b_{12}^{\gamma} &= (s_{33}s_{12} - s_{13}s_{23})/\delta_1, & b_{22}^{\gamma} &= s_{22} - s_{21}b_{12} - s_{23}b_{23},\\
b_{13}^{\gamma} &= -s_{13}/\delta_1, & b_{16}^{\gamma} &= (s_{33}d_{31} - s_{13}d_{33})/\delta_1, & b_{26}^{\gamma} &= d_{32} - s_{21}b_{16} - s_{23}b_{36},\\
b_{33}^{\gamma} &= s_{11}/\delta_1, & b_{23}^{\gamma} &= (s_{11}s_{23} - s_{13}s_{12})/\delta_1, & b_{66}^{\gamma} &= \epsilon_{33} - d_{31}b_{16} - d_{33}b_{36},\\
b_{44}^{\gamma} &= s_{44}, & b_{36}^{\gamma} &= (s_{11}d_{33} - s_{13}d_{31})/\delta_1, & b_{t1}^{\gamma} &= (-s_{33}\alpha_1 + s_{13}\alpha_3)/\delta_1,\\
b_{55}^{\gamma} &= s_{66}, & b_{t2}^{\gamma} &= (s_{21}b_{t1} + s_{23}b_{t3} + \alpha_2), & b_{t3}^{\gamma} &= (-s_{11}\alpha_3 + s_{13}\alpha_1)/\delta_1,\\
\delta_1 &= s_{33}s_{11} - s_{13}^2, & b_{t6}^{\gamma} &= d_{31}b_{t1} + d_{33}b_{t3} + q_3.
\end{aligned} \tag{13}$$

Substituting (13) for $\gamma = p$ and m into (11) and applying (10) yields

$$\bar{V}^b = (v_2^p B^p + v_2^m B^m)\bar{U}^b + (v_2^p B_t^p + v_2^m B_t^m)\bar{T} = \bar{B}\bar{U}^b + \bar{B}_t\bar{T}. \tag{14}$$

Rewriting (14) in the original form of (1) yields the effective constitutive equation for model B as

$$\begin{bmatrix} \bar{\varepsilon}_1 \\ \bar{\varepsilon}_2 \\ \bar{\varepsilon}_3 \\ \bar{\gamma}_{23} \\ \bar{\gamma}_{12} \\ \bar{D}_3 \end{bmatrix} = \begin{bmatrix} s_{11} & s_{12} & s_{13} & 0 & 0 & d_{31} \\ s_{12} & s_{22} & s_{23} & 0 & 0 & d_{32} \\ s_{13} & s_{23} & s_{33} & 0 & 0 & d_{33} \\ 0 & 0 & 0 & s_{44} & 0 & 0 \\ 0 & 0 & 0 & 0 & s_{66} & 0 \\ d_{31} & d_{32} & d_{33} & 0 & 0 & \epsilon_{33} \end{bmatrix}^B \begin{bmatrix} \bar{\sigma}_1 \\ \bar{\sigma}_2 \\ \bar{\sigma}_3 \\ \bar{\tau}_{23} \\ \bar{\tau}_{12} \\ \bar{E}_3 \end{bmatrix} + \begin{bmatrix} \alpha_1 \\ \alpha_2 \\ \alpha_3 \\ 0 \\ 0 \\ q_3 \end{bmatrix}^B \bar{T}, \tag{15}$$

where the effective coefficients for model B are obtained as

$$\begin{aligned}
s_{11}^B &= \bar{b}_{33}/\delta_2, & s_{44}^B &= \bar{b}_{44}, & s_{12}^B &= (\bar{b}_{33}\bar{b}_{12} - \bar{b}_{13}\bar{b}_{23})/\delta_2, & s_{13}^B &= -\bar{b}_{13}/\delta_2,\\
s_{33}^B &= \bar{b}_{11}/\delta_2, & s_{66}^B &= \bar{b}_{55}, & s_{22}^B &= \bar{b}_{22} + s_{23}^B\bar{b}_{23} + s_{12}^B\bar{b}_{12}, & s_{23}^B &= (-\bar{b}_{12}\bar{b}_{13} + \bar{b}_{23}\bar{b}_{11})/\delta_2,\\
d_{31}^B &= (-\bar{b}_{36}\bar{b}_{13} + \bar{b}_{16}\bar{b}_{33})/\delta_2, & d_{32}^B &= \bar{b}_{26} + d_{31}^B\bar{b}_{12} + d_{33}^B\bar{b}_{23}, & d_{33}^B &= (-\bar{b}_{16}\bar{b}_{13} + \bar{b}_{36}\bar{b}_{11})/\delta_2,\\
\delta_2 &= \bar{b}_{33}\bar{b}_{11} - \bar{b}_{13}^2, & q_3^B &= \bar{b}_{16}\alpha_1^B + \bar{b}_{36}\alpha_3^B + \bar{b}_{t6}, & \epsilon_{33}^B &= \bar{b}_{66} + d_{31}^B\bar{b}_{16} + d_{33}^B\bar{b}_{36},\\
\alpha_1^B &= (-\bar{b}_{33}\bar{b}_{t1} + \bar{b}_{13}\bar{b}_{t3})/\delta_2, & \alpha_2^B &= \bar{b}_{21}\alpha_1^B + \bar{b}_{23}\alpha_3^B + \bar{b}_{t2}, & \alpha_3^B &= (\bar{b}_{13}\bar{b}_{t1} - \bar{b}_{11}\bar{b}_{t3})/\delta_2,
\end{aligned} \tag{16}$$

2.4. ***Combined model.*** For the case of the combined model AB, the material properties of the piezoelectric fiber phase in model B are replaced with the effective properties from model A. Since the shear stresses are uncoupled, it is readily possible to obtain the closed-form expressions for the effective s_{44} and s_{66} from model AB using (9) and (16) as

$$s_{44}^{AB} = v_f s_{44}^p + v_m s_{44}^m, \qquad s_{66}^{AB} = \frac{v_2^p s_{66}^p s_{66}^m + v_2^m s_{66}^m (v_3^p s_{66}^m + v_3^m s_{66}^p)}{(v_3^p s_{66}^m + v_3^m s_{66}^p)}, \tag{17}$$

where $v_f = v_2^p v_3^p$, $v_m = 1 - v_f$. Similarly, s_{55}^{AB} can be obtained as

$$s_{55}^{AB} = \frac{(v_3^p s_{55}^p + v_3^m s_{55}^m)s_{55}^m}{v_2^p s_{55}^m + v_2^m (v_2^p s_{55}^m + v_2^m s_{55}^p)}. \tag{18}$$

Usually v_2^p is taken as equal to v_3^p, in which case $v_2^p = v_3^p = \sqrt{v_f}$, where v_f is the overall volume fraction of fiber.

For fiber and matrix phases which are transversely isotropic about the fiber direction x_1, the effective material properties of the combined model should exhibit transverse isotropy. However, it can be seen from (17) and (18) that s_{66}^{AB} and s_{55}^{AB} will not be equal for this case. A similar inequality is observed among the other pairs of effective constants such as s_{12} and s_{13}, and s_{22} and s_{33}, which should also be equal for the transversely isotropic case. This discrepancy exists in the electromechanical micromechanics model of [Bent 1994]. To eliminate it, the effective properties of the combined model BA are obtained by replacing the properties of the fiber phase of model A with the effective properties from model B. The final effective properties P_i^e are then obtained by averaging those of models AB and BA:

$$P_i^e = (P_i^{AB} + P_i^{BA})/2. \tag{19}$$

While the expression for s_{44}^{BA} is the same as for model AB given in (17), the expressions for s_{55}^{BA} and s_{66}^{BA} are obtained by interchanging their expressions for model AB given by (17) and (18).

2.5. ***Thermal conductivity.*** The 3D heat conduction, according to Fourier's law, is governed by

$$Q_i = -k_i T_{,i} \quad \text{for} \quad i = 1, 2, 3, \tag{20}$$

where k_i, Q_i, and $T_{,i}$ denote respectively the thermal conductivities, heat flux, and temperature gradient along the x_i direction. To obtain the effective thermal conductivities using the isofield method, the temperature gradients parallel to the connecting plane of two phases and the heat flux along the normal to the connecting plane are assumed to be uniform over the two phases. The remaining complementary field variables are averaged over the two phases. For models A and B, this yields:

Model A:

$$\begin{aligned} \bar{H}^a &= H_p^a = H_m^a, & H^a &= \left[T_{,1},\, T_{,2},\, Q_3\right]^{\mathrm{T}}, \\ \bar{M}^a &= v_3^p M_p^a + v_3^m M_m^a, & M^a &= \left[Q_1,\, Q_2,\, T_{,3}\right]^{\mathrm{T}}. \end{aligned} \tag{21}$$

Model B:

$$\begin{aligned} \bar{H}^b &= H_p^b = H_m^b, & H^b &= \left[T_{,1},\, Q_2,\, T_{,3}\right]^{\mathrm{T}}, \\ \bar{M}^b &= v_3^p M_p^b + v_3^m M_m^b, & M^b &= \left[Q_1,\, T_{,2},\, Q_3\right]^{\mathrm{T}}. \end{aligned} \tag{22}$$

Using (20), the dependent variables M_γ^a and M_γ^b ($\gamma = p, m$) are expressed, respectively, in terms of the independent variables H_γ^a and H_γ^b, and the resulting equations are arranged in the form of (20), to yield the effective thermal conductivities for models A and B. As before, the effective thermal conductivities k_i^{AB} of the combined model AB are then obtained by using the effective thermal conductivities obtained from model A in model B as the conductivities of its fiber phase, which yields

$$k_1^{AB} = v_f k_1^p + v_m k_1^m, \quad k_2^{AB} = \frac{v_3^p k_2^p k_2^m + v_3^m (k_2^m)^2}{v_2^p k_2^m + v_2^m (v_3^p k_2^p + v_3^m k_2^m)}, \quad k_3^{AB} = \frac{v_2^p k_3^p k_3^m + v_2^m k_3^m (k_3^m v_3^p + v_3^m k_3^p)}{v_3^p k_3^m + v_3^m k_3^p}. \tag{23}$$

In the combined model BA, the expression for the effective k_1 is the same as for model AB, and the expressions for the effective k_2 and k_3 get interchanged. The final effective k_i^e are obtained using (19).

3. Results and discussion

Numerical results for the effective thermoelectroelastic properties are presented for two PFRC systems made, respectively, of PZT-7A and PZT-5H fibers and an epoxy matrix. The material properties of the fibers and the matrix are listed in Table 1. The following nondimensional parameters are introduced to compare the effective properties of the PFRC materials with the corresponding piezoelectric fibers:

$$R^e_{3i} = \frac{e^e_{3i}}{e^p_{3i}}, \qquad R^d_{3i} = \frac{d^e_{3i}}{d^p_{3i}}, \qquad \bar{\alpha}_i = \frac{\alpha^e_i}{\alpha^p_i}, \qquad \bar{k}_i = \frac{k^e_i}{k^p_i} \quad \text{for } i = 1, 2, 3;$$

$$\bar{s}_{ij} = \frac{s^e_{ij}}{s^p_{ij}} \quad \text{for } i = 1, 2, 6; \qquad R^{\epsilon}_{33} = \frac{\epsilon^e_{33}}{\epsilon^p_{33}}, \qquad R^q_3 = \frac{q^e_3}{q^p_3}.$$

The effective elastic stiffness constants c^e_{ij} of the PZT-7A/epoxy system are plotted in Figure 3 against the fiber volume fraction v_f and compared with those predicted by [Ray 2006]. Due to two-way electromechanical coupling, the effective stiffness is affected by the piezoelectric coupling constants d_{ij}. In order to ascertain this effect, the elastic constants c^e_{ij} computed considering $d_{ij} = 0$ are also compared in Figure 3. It is observed that the electromechanical coupling has a stiffening effect on PFRC resulting in greater values for constants c^e_{11}, c^e_{33}, and c^e_{12}. While the c^e_{11} predicted by [Ray 2006] match closely with the present estimate with $d_{ij} = 0$, there are appreciable differences between the two results for c^e_{33}, c^e_{12}, and c^e_{23}. The difference increases for all constants, when the d_{ij} are not considered zero in the present model.

The variations of nondimensional effective piezoelectric stress constants R^e_{3i} with fiber volume fraction are plotted in Figure 4 for the same PFRC system for different values of the dielectric ratio (DR $= \epsilon^p_{33}/\epsilon^m_{33}$). The DR was varied by varying the matrix property (ϵ^m_{33}) keeping the fiber property fixed. The case of DR $= 1$ leads to uniform electric field E_3 across both fiber and matrix phases, a condition assumed by

Material	c_{11}	c_{22}	c_{33}	c_{12}	c_{23}	c_{31}	c_{44}	c_{55}	c_{66}
PZT-7A[1]	148	148	131	76.2	74.2	74.2	25.4	25.4	35.9
PZT-5H[2]	126	126	117	79.5	84.1	84.1	23	23	23.25
epoxy[1]	3.86	3.86	3.86	2.57	2.57	2.57	0.645	0.645	0.645
	e_{31}	e_{32}	e_{33}	e_{14}	e_{24}			ϵ_{33}	
PZT-7A[1]	–2.1	–2.1	9.5	9.2	9.2			2.07	
PZT-5H[2]	–6.5	–6.5	23.3	17	17			30.42	
epoxy[1]	0	0	0	0	0			0.079	
	α_1	α_2	α_3	k_{11}	k_{22}	k_{33}		p_3	
PZT-7A[1]	1	1	1	–	–	–		2	
PZT-5H[3]	9.64	9.64	3.96	50	50	75		5.483	
epoxy[1,4]	24	24	24	0.18	0.18	0.18		0.0	

Table 1. Material properties: c_{ij} in GPa, e_{ij} in $\mathrm{C\,m^{-2}}$, ϵ_{33} in $10^{-9}\,\mathrm{C\,V^{-1}\,m^{-1}}$, α_i in $10^{-6}\,\mathrm{K^{-1}}$, k_{ij} in $\mathrm{W\,K^{-1}\,m^{-1}}$, p_i in $10^{-5}\,\mathrm{C\,m^2\,K^{-1}}$.
[1] [Kumar and Chakraborty 2009] [2] [Kapuria and Hagedorn 2007] [3] [Chen 2006]
[4] [Gibson 2007, Table 3.2, p. 106].

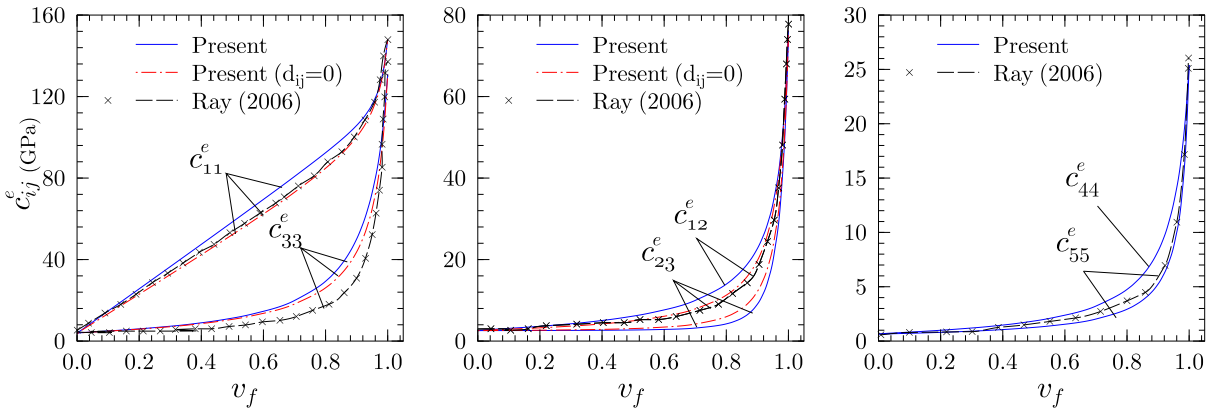

Figure 3. Variation of effective stiffness constants of PZT-7A/epoxy with fiber volume fraction.

[Ray 2006]. While the value of R^e_{31} predicted by the present model for DR = 1 is in close agreement with the reference solution, values of R^e_{32} and R^e_{33} predicted by the later model are much lower than the present solution. In the present model, ε_2 and σ_3 are uniform over two phases in model A, while σ_2 and ε_3 are uniform in model B, according to the respective connecting planes, which are consistent with the actual boundary conditions of the RVE. However, in the model of [Ray 2006], both σ_2 and σ_3 are assumed to have a uniform variation over the two phases, simultaneously. This explains the difference between the two results even though both correspond to the uniform electric field case. Figure 4 also reveals that the effective piezoelectric constants of PFRC are highly sensitive to the DR and reduce drastically with its increase. This is because the ratio of electric field across the fiber phase to that applied across the PFRC thickness decreases with the increase in DR. Even though both constituents exhibit transverse isotropy about axis x_3, effective values of e_{31} and e_{32} differ, since the connectivity between the fiber and matrix phases does not follow symmetry about axis x_3. This difference between e_{31} and e_{32} in PFRC enables directional (anisotropic) in-plane actuation, which is desirable in many control applications. The effective thermal stress coefficients β_1 and β_3 for the PZT-7A/epoxy system for varying v_f, computed with and without making $d_{ij} = 0$, are compared with those of [Kumar and Chakraborty 2009] in Figure 5. Once again, the present results match with the reference solution, when computed with $d_{ij} = 0$, but otherwise differ considerably for intermediate values of v_f.

In Figures 6 and 7, nondimensionalized compliances ($\bar{s}_{11}$, $\bar{s}_{12}$, $\bar{s}_{66}$) and coefficients of thermal expansion ($\bar{\alpha}_1$, $\bar{\alpha}_2$) are compared with the simple rule of mixtures (ROM)/inverse rule of mixtures (IROM) and the modified rule of mixtures (MROM) given in Appendix B. The effective values of the thermoelastic constants predicted by the present model are close to those predicted by the ROM for longitudinal constants s^e_{11} and α^e_1 and by the MROM for the transverse constants s^e_{66} and α^e_2, but are not so for the transverse compliance constants s^e_{22} and s^e_{33}. The nondimensionalized effective thermal conductivities $\bar{k}^e_1$ and $\bar{k}^e_3$ are also plotted in Figure 7.

The variations of the ratios R^d_{3i} $(i = 1, 2, 3)$ of effective values of piezoelectric strain constants d_{3i} to the corresponding values for the bulk PZT are plotted in Figure 8 for both PZT-7A/epoxy and PZT-5H/epoxy systems for different values for DR ranging from 1 to 100. Similar to constants e_{3i}, the effective values of d_{3i} are maximum for DR = 1, when the electric field is uniform across piezoelectric and matrix phases, and decrease sharply with the increase in DR, as happens for commonly used matrix materials. Even

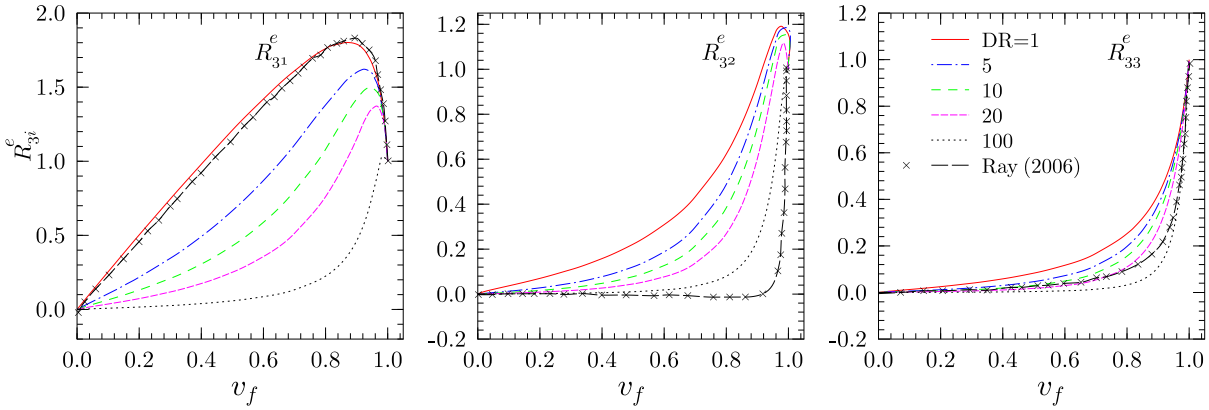

Figure 4. Variation of effective piezoelectric stress constant ratios of PZT-7A/epoxy with fiber volume fraction.

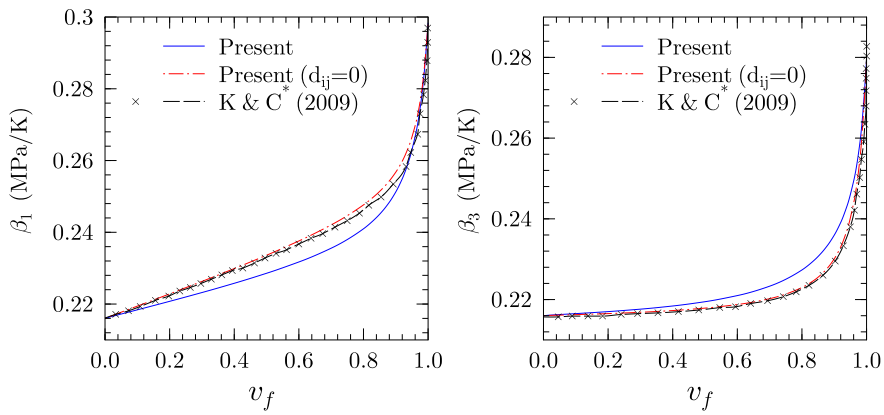

Figure 5. Variation of effective thermal stress coefficients of PZT-7A/epoxy with fiber volume fraction.

* [Kumar and Chakraborty 2009].

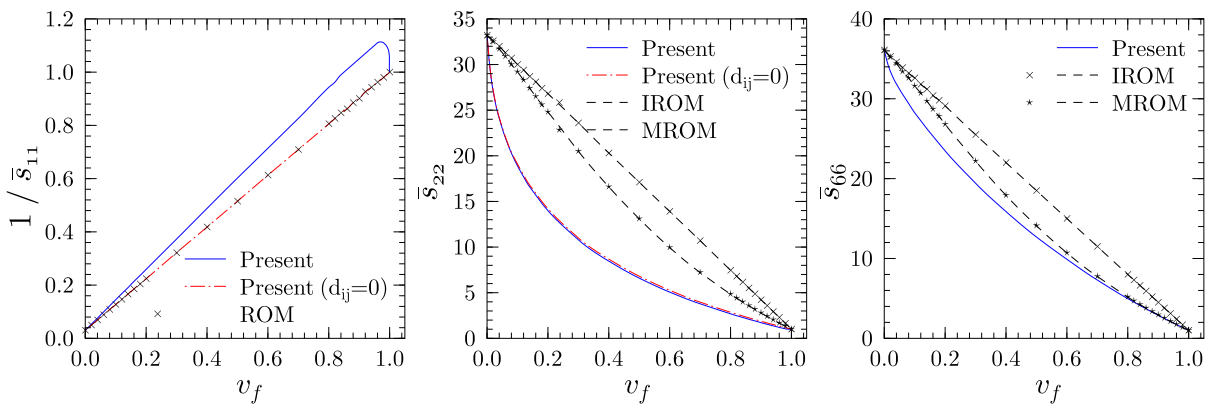

Figure 6. Variation of effective compliance coefficients of PZT-5H/epoxy with fiber volume fraction.

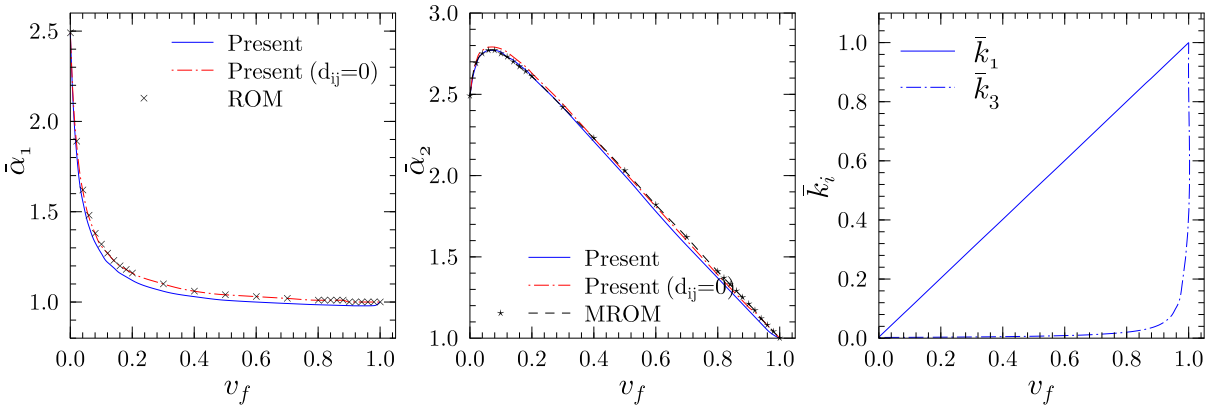

Figure 7. Variation of effective thermal expansion coefficients and conductivities of PZT-5H/epoxy with fiber volume fraction.

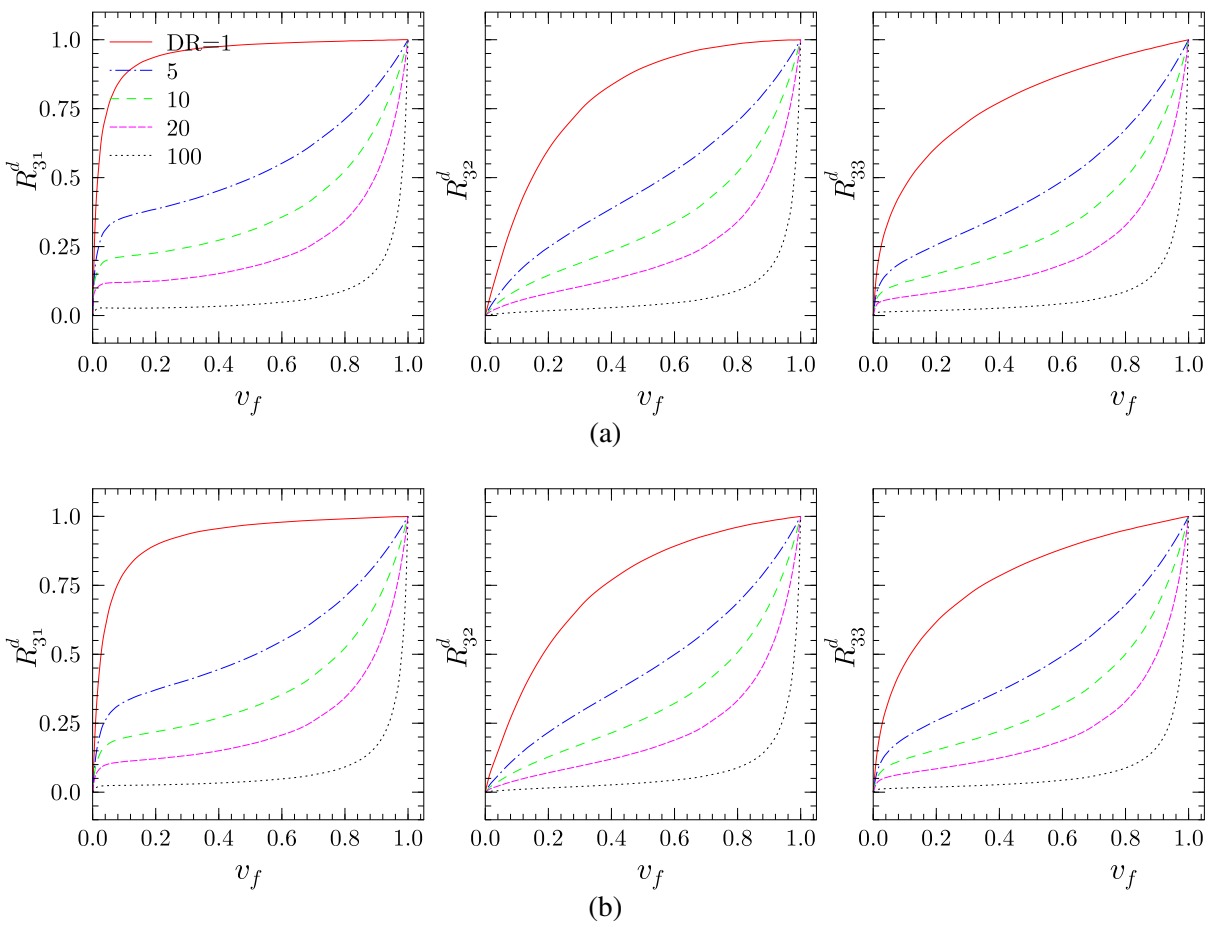

Figure 8. Effect of DR on effective piezoelectric strain constants of PFRCs, for (a) PZT-7A/epoxy and (b) PZT-5H/epoxy.

at a low fiber volume fraction of 10%, there is a large difference between the results of d_{3i}^e at DR = 1 and DR = 5. This is because the electric field E_3^p across the piezoelectric phase in model A is only a fraction of the overall electric field $\bar{E}_3$ and is dependent on both v_3^p and DR. For example, ignoring the electromechanical coupling, E_3^p in model A can be easily obtained, using (2)–(8), as

$$\frac{E_3^p}{\bar{E}_3} = \frac{1}{v_3^p + v_3^m(\mathrm{DR})}.$$

Thus, E_3^p is more sensitive to DR at a lower value of the fiber volume fraction. The performance of these PFRCs can thus be improved either by using suitable matrix materials with dielectric constant ϵ_{33}^m of the order of ϵ_{33}^p or by directly applying electric fields across the piezoelectric fibers. It is also revealed from Figure 8 that above 90% of the value of d_{31} of the bulk PZT can be achieved in the PFRC with a fiber volume fraction of only 25% for the uniform field case. While the values of effective piezoelectric strain constants d_{3i}^e vary from zero to those of the piezoelectric fibers, the effective values of piezoelectric stress constants e_{3i} can exceed those of the bulk piezoelectric material at an intermediate value of v_f (Figure 4). The latter leads to an impression that a higher electromechanical coupling can be achieved in PFRC than the bulk piezoelectric material [Ray 2006], which is clearly not true. Thus, the fundamental constants d_{ij} (and not e_{ij}) should be used for evaluating the effective electromechanical coupling property of PFRC.

The variations of nondimensionalized effective dielectric and pyroelectric constants with v_f are plotted in Figure 9. The effective pyroelectric constant almost follows the ROM for DR of unity, but

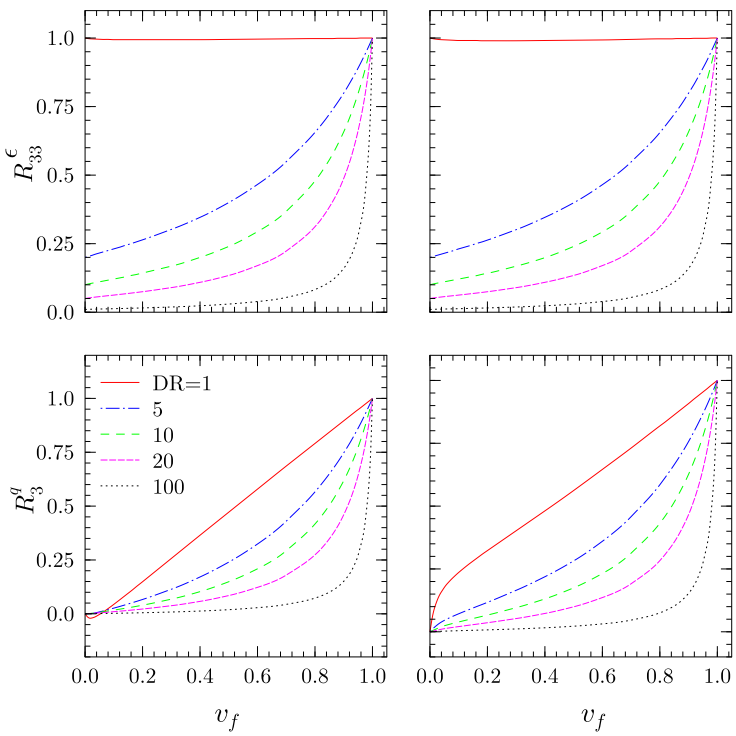

Figure 9. Variation of effective dielectric and pyroelectric constants of PFRCs with fiber volume fraction: PZT-7A/epoxy (left column) and PZT-5H/epoxy (right column).

	PZT-5H/epoxy				PZT-7A/epoxy			
Entity	0.2	0.4	0.6	0.8	0.2	0.4	0.6	0.8
s^e_{11}	65.12	34.76	23.91	18.56	43.25	22.59	15.39	11.83
s^e_{22}	233.7	141.3	85.06	45.60	222.8	132.8	77.99	39.37
s^e_{33}	225.1	135.1	80.58	43.16	212.6	125.3	72.20	35.28
s^e_{12}	–30.39	–16.63	–11.27	–8.15	–21.75	–11.66	–7.79	–5.61
s^e_{13}	–20.84	–10.33	–7.08	–6.07	–10.73	–4.39	–2.60	–2.11
s^e_{23}	–89.88	–39.37	–17.06	–8.07	–86.29	–35.26	–13.16	–4.28
s^e_{44}	1250	950	650	345	1250	950	640	340
s^e_{55}	1010	680	420	215	1010	680	420	210
s^e_{66}	1010	680	420	214	1000	670	410	200
d^e_{31}	–33.15	–41.25	–57.01	–94.32	–5.24	–6.39	–8.88	–15.14
d^e_{32}	–19.33	–33.07	–51.94	–91.40	–3.36	–5.48	–8.45	–14.99
d^e_{33}	50.38	73.52	111.2	195.3	8.72	12.70	19.56	35.81
ϵ^e_{33}	2.27	3.30	5.16	9.49	0.12	0.18	0.28	0.53
q^e_3	–0.99	–2.00	–3.74	–7.78	0.44	1.15	2.47	5.71
α^e_1	11.07	10.24	9.94	9.77	3.09	2.19	1.84	1.59
α^e_2	25.33	21.53	17.46	13.48	25.12	19.06	12.93	7.01
α^e_3	22.02	17.03	12.32	7.96	24.12	17.55	11.23	5.40
k^e_1	11.20	20.90	30.60	40.30	1.56	1.62	1.68	1.74
k^e_2	0.78	1.18	1.95	4.14	0.63	0.80	1.01	1.33
k^e_3	0.79	1.19	1.97	4.26	0.63	0.80	1.01	1.33

Table 2. Effective electrothermoelastic properties for PFRCs: s^e_{ij} in $10^{-12}\,\mathrm{Pa}^{-1}$, d^e_{3j} in $\mathrm{pm\,V}^{-1}$, ϵ^e_{33} in $\mathrm{nF\,m}^{-1}$, q^e_3 in $\mu\mathrm{C\,m}^{-2}\,\mathrm{K}^{-1}$, α^e_i in $10^{-6}\,\mathrm{K}^{-1}$, k^e_i in $\mathrm{W\,m}^{-1}\,\mathrm{K}^{-1}$.

drops sharply as the DR increases. Effective material properties for PZT-5H/epoxy with DR = 20 and PZT-7A/epoxy with DR = 26.2 are presented in Table 2 for four values of the fiber volume fraction ($v_f = 0.2, 0.4, 0.6, 0.8$). These properties are directly useful for 1D/2D/3D thermoelectromechanical analysis of smart laminated structures integrated with these PFRCs.

4. Conclusions

A coupled 3D isofield-based micromechanical model is presented for calculating effective electrothermoelastic properties of piezoelectric fiber-reinforced composite (PFRC) materials with poling and electric field applied along the normal to the fiber direction. The model employs the isofield method on representative volume elements (RVEs) of two possible connectivities, A and B, for the fiber and matrix phases. The two RVEs are combined in sequences AB and BA, so as to achieve transverse isotropy in the effective properties when both the constituents are transversely isotropic. The model considers differential electric fields in fiber and matrix phases due to their different dielectric constants. The assumption of uniform electric field across the two phases made by some existing theories can be achieved as a special case of the present formulation when the dielectric ratio (DR) is unity.

Results presented for two PFRC systems, PZT-7A/epoxy and PZT-5H/epoxy, reveal that it is possible to achieve effective piezoelectric strain constant d_{31} of magnitude greater than 90% of that of bulk piezoelectric material with even a low fiber volume fraction of 25%, if the DR is close to unity. The effective piezoelectric constants, however, reduce drastically as the DR increases. While the magnitudes of effective d_{3i} of PFRC vary from zero to those of the piezoelectric fiber, the effective e_{3i} can exceed its value for the fiber at an intermediate value of v_f, giving a false notion of improved performance, for DR close to unity. Therefore, constants d_{ij} should be used to evaluate electromechanical coupling of PFRCs. The effective pyroelectric constant nearly follows the rule of mixtures for DR of unity, but reduces as DR increases.

Appendix A

The isofield micromechanics model, also known as the uniform field model, is basically a generalization of the strength of materials approach of estimating overall properties of two-phase composite materials. The basic assumption, as the name implies, is that all fields are uniform within each material phase. This assumption makes the model independent of the geometry of its microstructure, and it is possible to refer to the two phases in a RVE as two cuboidal blocks connected at a plane. This forms the basis of the RVE representation in Figure 2. The model actually violates some of the compatibility and equilibrium conditions at the interface. However, it has been successfully used in the past (see, for example, [Jones 1975]) for estimating mechanical and transport (conductivity, thermal expansion coefficient) properties of fiber-reinforced composite materials. The large mismatch in the material properties makes the method particularly well suited for modeling such fibrous composites. Its accuracy largely depends on the spatial scale of the phase distributions. For finely distributed phases, it is expected to yield good estimates of the averaged response. A major advantage of this method is that it provides simple analytical solutions for the effective properties, which allows physical insight into the problem.

For uniaxial fields, the uniform field assumption leads to the well-known rules of mixtures, comprising of parallel and series (Voigt and Reuss) additions for estimating the effective properties along and perpendicular to the fiber direction, respectively. For the 3D fields, however, it is not as straightforward. Typically, the conventional model with parallel connectivity yields very good estimates of longitudinal properties, but the series model at best yields a lower bound of the transverse properties. This is improved by using a combination model, wherein the two phases in the RVE are connected at two orthogonal planes (x_1-x_2 and x_1-x_3) parallel to the fiber direction (x_1), instead of only one plane as in the conventional model, as shown in Figure 2 (combined model). The combination model is treated as follows: blocks of piezoelectric (p) and matrix (m) phases are connected at the x_1-x_2 plane and they together are connected to a matrix phase at the x_1-x_3 plane, and vice versa. Thus, models A and B with the two phases connected at the x_1-x_2 and x_1-x_3 planes, respectively, form the building blocks of the combination model.

The other assumptions in the present model are that

- the two material phases are perfectly bonded,
- deformation and electric fields are small enough that linear constitutive equations can be applied, and
- the piezoelectric materials are uniformly polarized along the x_3 direction.

Appendix B

The expressions for the effective Young's moduli Y_i^e, shear modulus G_{12}^e, and thermal expansion coefficients α_i^e according to the rule of mixtures (ROM)/inverse rule of mixtures (IROM) and the modified rule of mixtures (MROM) based on the strength of materials approach can be found in [Gibson 2007]. These are given below:

- ROM/IROM

$$Y_1^e = Y_1^p v_f + Y_1^m v_m, \qquad \alpha_1^e = \frac{Y_1^p \alpha_1^p v_f + Y_1^m \alpha_1^m v_m}{Y_1^p v_f + Y_1^m v_m},$$

$$\frac{1}{Y_2^e} = \frac{v_f}{Y_2^p} + \frac{v_m}{Y_2^m}, \qquad \frac{1}{G_{12}^e} = \frac{v_f}{G_{12}^p} + \frac{v_m}{G_{12}^m}.$$

- MROM

$$Y_2^e = Y_2^m \left[(1 - \sqrt{v_f}) + \frac{\sqrt{v_f}}{1 - \sqrt{v_f}(1 - Y_2^m / Y_2^p)} \right],$$

$$G_{12}^e = G_{12}^m \left[(1 - \sqrt{v_f}) + \frac{\sqrt{v_f}}{1 - \sqrt{v_f}(1 - G_{12}^m / G_{12}^p)} \right],$$

$$\alpha_2^e = (1 + \nu_m)\alpha_2^m v_m + (1 + \nu_p)\alpha_2^p v_f - \alpha_1 \nu_{12}^e, \quad \text{where} \quad \nu_{12}^e = \nu_{12}^p v_f + \nu^m v_m.$$

Acknowledgements

Part of this work was done during the Kapuria's visit to the Division of Mechanics and Computation, Department of Mechanical Engineering, Stanford University, as a Fulbright–Nehru Senior Research Fellow. The author is thankful to the Fulbright Foundation for the grant and to his host, Professor Charles R. Steele, for his kind support. The first author expresses his gratitude to Marie-Louise Steele, then Associate Editor of JoMMS, for her encouragement and support during the application process for the fellowship, just before her tragic illness.

References

[Aboudi 1998] J. Aboudi, "Micromechanical prediction of the effective coefficients of thermo-piezoelectric multiphase composites", *J. Intell. Mater. Syst. Struct.* **9**:9 (1998), 713–722.

[Auld 1973] B. A. Auld, *Acoustic fields and waves in solids*, vol. 1, Wiley, New York, 1973.

[Bent 1994] A. A. Bent, "Piezoelectric fiber composites for structural actuation", Master's thesis, Massachusetts Institute of Technology, Cambridge, MA, 1994, Available at http://hdl.handle.net/1721.1/12322.

[Chan and Unsworth 1989] H. L. W. Chan and J. Unsworth, "Simple model for piezoelectric ceramic/polymer 1-3 composites used in ultrasonic transducer applications", *IEEE Trans. Ultrason. Ferroelectr. Freq. Control* **36**:4 (1989), 434–441.

[Chen 2006] C.-D. Chen, "On the singularities of the thermo-electro-elastic fields near the apex of a piezoelectric bonded wedge", *Int. J. Solids Struct.* **43**:5 (2006), 957–981.

[Chopra 2002] I. Chopra, "Review of state of art of smart structures and integrated systems", *AIAA J.* **40**:11 (2002), 2145–2187.

[Dong et al. 2006] X.-J. Dong, G. Meng, and J.-C. Peng, "Vibration control of piezoelectric smart structures based on system identification technique: numerical simulation and experimental study", *J. Sound Vib.* **297**:3–5 (2006), 680–693.

[Dunn and Taya 1993] M. L. Dunn and M. Taya, "Micromechanics predictions of the effective electroelastic moduli of piezoelectric composites", *Int. J. Solids Struct.* **30**:2 (1993), 161–175.

[Gibson 2007] R. F. Gibson, *Principles of composite material mechanics*, 2nd ed., CRC Press, Boca Raton, FL, 2007.

[Jones 1975] R. M. Jones, *Mechanics of composite materials*, Hemisphere, New York, 1975.

[Kapuria and Hagedorn 2007] S. Kapuria and P. Hagedorn, "Unified efficient layerwise theory for smart beams with segmented extension/shear mode, piezoelectric actuators and sensors", *J. Mech. Mater. Struct.* **2**:7 (2007), 1267–1298.

[Kapuria and Kumari 2010] S. Kapuria and P. Kumari, "Three-dimensional piezoelasticity solution for dynamics of cross-ply cylindrical shells integrated with piezoelectric fiber reinforced composite actuators and sensors", *Compos. Struct.* **92**:10 (2010), 2431–2444.

[Kar-Gupta and Venkatesh 2005] R. Kar-Gupta and T. A. Venkatesh, "Electromechanical response of 1-3 piezoelectric composites: effect of poling characteristics", *J. Appl. Phys.* **98**:5 (2005), 054102.

[Kumar and Chakraborty 2009] A. Kumar and D. Chakraborty, "Effective properties of thermo-electro-mechanically coupled piezoelectric fiber reinforced composites", *Mater. Des.* **30**:4 (2009), 1216–1222.

[Levin et al. 2000] V. M. Levin, T. Michelitsch, and I. Sevostianov, "Spheroidal inhomogeneity in a transversely isotropic piezoelectric medium", *Arch. Appl. Mech.* **70**:10 (2000), 673–693.

[Levin et al. 2008] V. M. Levin, F. J. Sabina, J. Bravo-Castillero, R. Guinovart-Díaz, R. Rodríguez-Ramos, and O. C. Valdiviezo-Mijangos, "Analysis of effective properties of electroelastic composites using the self-consistent and asymptotic homogenization methods", *Int. J. Eng. Sci.* **46**:8 (2008), 818–834.

[Mallik and Ray 2003] N. Mallik and M. C. Ray, "Effective coefficients of piezoelectric fiber-reinforced composites", *AIAA J.* **41**:4 (2003), 704–710.

[Park et al. 2010] S. Park, C. Lee, and H. Sohn, "Reference-free crack detection using transfer impedances", *J. Sound Vib.* **329**:12 (2010), 2337–2348.

[Ray 2006] M. C. Ray, "Micromechanics of piezoelectric composites with improved effective piezoelectric constant", *Int. J. Mech. Mater. Des.* **3**:4 (2006), 361–371.

[Sabina et al. 2001] F. J. Sabina, R. Rodríguez-Ramos, J. Bravo-Castillero, and R. Guinovart-Díaz, "Closed-form expressions for the effective coefficients of a fibre-reinforced composite with transversely isotropic constituents, II: Piezoelectric and hexagonal symmetry", *J. Mech. Phys. Solids* **49**:7 (2001), 1463–1479.

[Smith and Auld 1991] W. A. Smith and B. A. Auld, "Modeling 1-3 composite piezoelectrics: thickness-mode oscillations", *IEEE Trans. Ultrason. Ferroelectr. Freq. Control* **38**:1 (1991), 40–47.

[Uchino 2000] K. Uchino, *Ferroelectric devices*, Marcel Dekker, New York, 2000.

Received 1 Apr 2010. Revised 21 Aug 2010. Accepted 27 Aug 2010.

SANTOSH KAPURIA: kapuria@am.iitd.ac.in
Department of Applied Mechanics, Indian Institute of Technology Delhi, Hauz Khas, New Delhi 110016, India
http://web.iitd.ac.in/~am/

POONAM KUMARI: kpmech.iitd@gmail.com
Department of Applied Mechanics, Indian Institute of Technology Delhi, Hauz Khas, New Delhi 110016, India